Bioorganic & Medicinal Chemistry 17 (2009) 8113–8122

Contents lists available at ScienceDirect

Bioorganic & Medicinal Chemistry

journal homepage: www.elsevier.com/locate/bmc

Antitumor antibiotic fostriecin covalently binds to cysteine-269 residue of protein phosphatase 2A catalytic subunit in mammalian cells

Toshifumi Takeuchi [a], Noriyuki Takahashi [a], Kazutomo Ishi [b], Tomoe Kusayanagi [a], Kouji Kuramochi [a], Fumio Sugawara [a,b,*]

[a] Department of Applied Biological Science, Tokyo University of Science (RIKADAI), 2641 Yamazaki, Noda-shi, Chiba 278-8510, Japan
[b] Genome and Drug Research Center, Tokyo University of Science (RIKADAI), 2641 Yamazaki, Noda-shi, Chiba 278-8510, Japan

ARTICLE INFO

Article history:
Received 3 September 2009
Revised 25 September 2009
Accepted 26 September 2009
Available online 3 October 2009

Keywords:
Fostriecin
Protein phosphatase 2A catalytic subunit
Covalent bond
α,β-Unsaturated lactone

ABSTRACT

Fostriecin is a phosphate monoester with excellent antitumor activity against mouse leukemia, and it is a potent inhibitor of protein phosphatase (PP) 2A. This compound has been predicted to covalently bind to the Cys269 residue of the PP2A catalytic subunit (PP2Ac) at the α,β-unsaturated lactone via a conjugate addition reaction. However, this binding has not yet been experimentally proven. To confirm such binding, we synthesized biotin-labeled fostriecin (bio-Fos), which has an inhibitory activity against the proliferation of mouse leukemia cells. We showed that fostriecin directly binds to PP2Ac in HeLa S3 cells by pull-down assays using bio-Fos. Moreover, we directly demonstrated that fostriecin covalently binds to the Cys269 residue of PP2Ac by matrix assisted laser desorption/ionization time-of-flight mass spectrometry analysis. From these results, the inhibitory mechanism of fostriecin on PP2A activity is discussed.

1. Introduction

Fostriecin (Fig. 1) is a phosphate monoester isolated in 1983 by Tunac and co-workers from a fermentation broth of *Streptomyces pulveraceus* subsp. *fostreus* ATCC 31906.[1–5] It exhibits antitumor activity against a wide spectrum of tumor cells in vitro and has excellent inhibitory activities against mouse leukemia cell lines L1210 and P388 in vivo.[6–10] Initially, its antitumor effect was suggested to be due to the inhibition of topoisomerase II.[11] However, fostriecin has recently been shown to interrupt a cellular mitotic entry checkpoint via a more potent and selective inhibition of the enzymatic activity of protein phosphatase (PP) 2A versus PP1 (inhibitory activity: PP1, IC_{50} = 45 μM; PP2A, IC_{50} = 1.5 nM; selectivity: PP2A/PP1 >10^4–10^5).[12–17] Thus, fostriecin is widely used as a selective PP2A inhibitor in studies of the phosphorylation signaling pathway.[18,19]

It has been reported that some biologically active compounds containing α,β-unsaturated carbonyl moiety can react with biological nucleophiles such as the sulfhydryl group of the cysteine residue.[20–25] Recently, we reported that monoacetylcurcumin, which selectively inhibits DNA polymerase λ, covalently binds to the cysteine residue of the BRCT domain in DNA polymerase λ.[25] The following previous reports have predicted that fostriecin covalently binds to the Cys269 residue of PP2Ac at the α,β-unsaturated lactone via conjugate addition: (1) The α,β-unsaturated δ-lactone of fostriecin has been observed for a potential Michael acceptor.[20–25] (2) The binding site of the Cys269 residue is unique to PP2A and PP4 and absent in PP1, PP2B, PP5 and PP7, and fostriecin selectively inhibits PP2A as against PP1 (>10^4–10^5),[15,27] PP2B (>10^5)[15] and PP5 (>10^4–10^5).[27] (3) The β12–β13 loop (256 VVTIF SAPNYCYRCG NQAAIMEL 278) of PP2Ac including the Cys269 residue (underlined) is essential for the inhibition of PP2Ac activity by fostriecin.[28] (4) PP2A C269S and C269F mutants in yeast are much less sensitive against fostriecin (>10).[28] (5) 2,3-Dihydrofostriecin has 200-fold less inhibitory activity against PP2A than fostriecin.[27] (6) Phoslactomycin, a member of the naturally occurring fostriecin family, has been reported to covalently bind to the Cys269 residue of PP2Ac, resulting in the selective inhibition of PP2A.[24] (7) Chimeras of PP1 and PP5, in which key residues predicted for inhibitor contact with PP2A (267 YRCG 270) were introduced into PP1 and PP5 using site-directed mutagenesis, are much more sensitive against fostriecin (>600 and ~200, respectively).[29] However, the covalent binding between fostriecin and PP2Ac has not yet been experimentally demonstrated.[24,26,29]

In this study, we investigated the covalent binding of fostriecin to PP2Ac in HeLa S3 cells by pull-down assays using synthetically prepared biotin-labeled fostriecin (bio-Fos). We were able to directly demonstrate that fostriecin covalently binds to the Cys269 residue of PP2Ac by matrix assisted laser desorption/ionization time-of-flight mass spectrometry (MALDI-TOF MS) analysis.

* Corresponding author. Tel.: +81 4 7124 1501x3400; fax: +81 4 7123 9757.
E-mail address: sugawara@rs.noda.tus.ac.jp (F. Sugawara).

0968-0896/$ - see front matter © 2009 Elsevier Ltd. All rights reserved.
doi:10.1016/j.bmc.2009.09.050

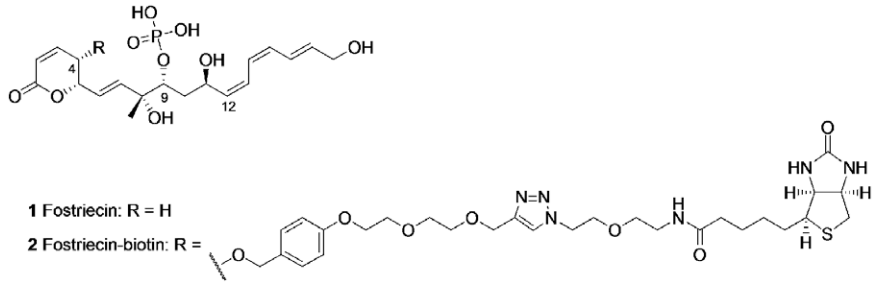

Figure 1. Structure of fostriecin (**1**) and biotin-labeled fostriecin (bio-Fos, **2**).

2. Results

2.1. Synthesis of biotin-labeled fostriecin

To identify the direct binding proteins of fostriecin by affinity matrix-based protein purification,[30–33] we chemically synthesized bio-Fos (Fig. 1). Synthesis started from the introduction of imidate **6** to alcohol (**12*Z***)-**7** (Scheme 1), which was reported in our previous work.[34] Imidate **6** was synthesized by the tosylation of commercially available alcohol **3**, followed by the alkylation of *p*-hydroxybenzyl alcohol with tosylate ester **4** to provide benzylic alcohol **5** in 56% yield over two steps, which was subsequently converted into imidate **6**. Treatment of alcohol (**12*Z***)-**7** with imidate **6** in the presence of triphenylmethyl (Tr) BF_4 furnished benzylic ether **8**, followed by the selective removal of the C8 triethylsilyl (TES) group to give alkyne **9** in 76% yield over two steps. For assembly of the probe molecule, biotin derivative **12** was prepared by the mono reduction of commercially available ether **10** and the subsequent condensation of the resulting amine with D-biotin. Huisgen cycloaddition[35–39] of alkyne **9** with azide **12**, followed by a Stille coupling reaction[40] of the resulting vinyl iodide **14** with the known stannane derivative **13**,[41,42] yielded triene **15** in 79% yield over three steps. After phosphorylation[43,44] of alcohol **15**, deprotection of the fluorenylmethyl and silyl group provided bio-Fos **2** as a triethylammonium salt in 36% yield over three steps.

2.2. Effects of biotin-labeled fostriecin on cell viability

The cytotoxicity of bio-Fos was evaluated on mouse leukemia cells. The 50% inhibitory concentration (IC_{50}) of bio-Fos was 58 μM (Fig. 2), as determined by WST-8 assay.[45,46] Although bio-Fos had weaker cytotoxic activity than fostriecin (IC_{50} = 0.46 μM),[10] it still retained cytotoxic activity toward the L1210 mouse leukemia cell line. Thus, we decided that **2** could be used for affinity matrix-based protein purification.

2.3. Fostriecin covalently binds to PP2Ac in HeLa S3 cells

We carried out pull-down assays using bio-Fos to confirm whether fostriecin covalently binds to PP2Ac.[24] HeLa S3 cells were incubated with 20 μM bio-Fos or biotin for 2 h. After washing with phosphate buffered saline (PBS), the cells were lysed. Both proteins

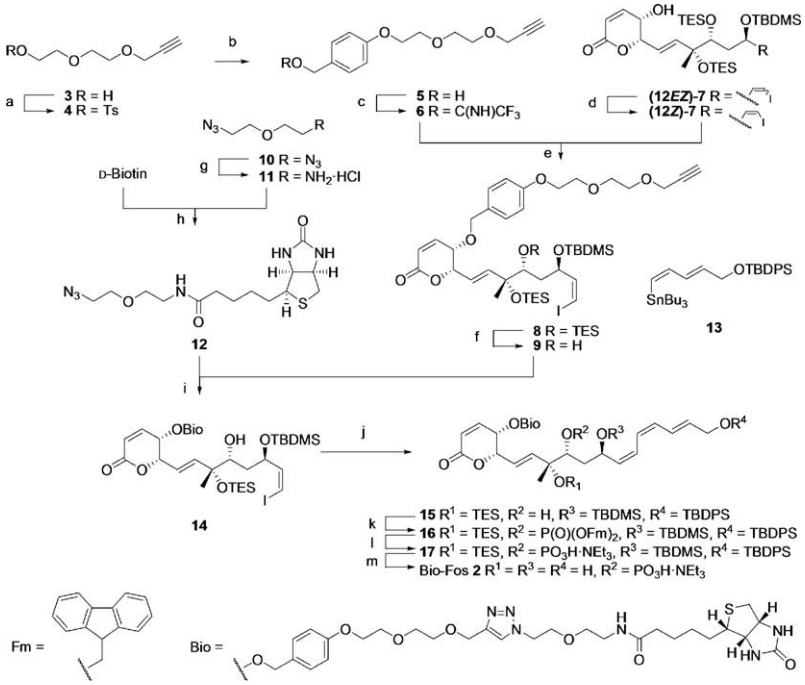

Scheme 1. Synthesis of bio-Fos (**2**). Reagents and conditions: (a) TsCl, DMAP/CH_2Cl_2 88%; (b) *p*-hydroxybenzyl alcohol, K_2CO_3/MeCN, 64%; (c) Cl_3CCN, NaH/CH_2Cl_2; (d) separation, 78%; (e) $TrBF_4/Et_2O$; (f) HCl aq, THF, MeCN, 69% in two steps; (g) PPh_3/EtOAc, HCl aq, 79%; (h) *i*-Pr_2NEt, HBTU/DMF, 89%; (i) CuI, Et_3N/THF, 98%; (j) **13**, $Pd(MeCN)_2Cl_2$/DMF, 81%; (k) *i*-$Pr_2NP(OFm)_2$, tetrazole/CH_2Cl_2 then TBHP; (l) Et_3N/MeCN; (m) $Et_3N{\cdot}3HF$, Et_3N/MeCN, 36%. Ts = *p*-toluenesulfonyl, DMAP = *N*,*N*-dimethy-4-laminopyridine, Tr = triphenylmethyl, THF = tetrahydrofuran, HBTU = *O*-benzotriazole-*N*,*N*,*N*′,*N*′-tetramethyl-uronium-hexafluoro-phosphate, DMF = *N*,*N*-dimethylformamide, TBHP = *tert*-butyl hydroperoxide.

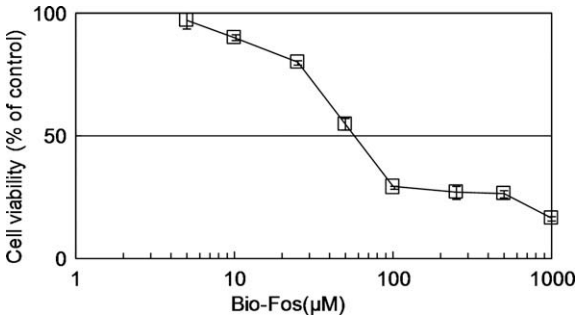

Figure 2. Dose-dependant effects of bio-Fos on L1210 cell viability as determined by WST-8 assay. Dose–response curve of growth inhibition induced by fostriecin-biotin (□) in L1210 cells. Data are presented as means ± SEM of three independent experiments.

binding to bio-Fos or biotin were precipitated with streptavidin beads and analyzed by sodium dodecyl sulfate polyacrylamide gel electrophoresis (Fig. 3A). Silver staining revealed the presence of several proteins in the sample derived from bio-Fos-treated cells (Fig. 3Aa, arrows). Detection of biotinylated proteins using alkaline phosphatase-conjugated avidin (AP-avidin) demonstrated a biotinylated 36 kDa protein in the sample from bio-Fos-treated cells (Fig. 3Ab, arrow). This protein was identified as PP2Ac by Western blot analysis using anti-PP2Ac antibody (Fig. 3Ac). This result indicates that PP2Ac was covalently biotinylated by bio-Fos addition, implying that bio-Fos covalently binds to PP2Ac in living cells.

To determine the binding specificity between bio-Fos and PP2Ac (Fig. 3B), we performed competition assay with fostriecin. After pretreatment of HeLa S3 cells with free fostriecin at several concentrations (0, 0.01, 0.1, and 1 μM) for 1.5 h, the cells were incubated with 20 μM bio-Fos or biotin for 1 h. Biotin-containing proteins were isolated with streptavidin beads and analyzed by Western blot analysis using AP-avidin and anti-PP2Ac antibody. The bands obtained from PP2Ac were reduced by the addition of fostriecin, indicating that the binding between bio-Fos and PP2Ac was competitively blocked by fostriecin in a dose-dependent manner. These observations strongly suggest that fostriecin competes with bio-Fos in the same binding site of PP2Ac.

2.4. Fostriecin covalently binds to Cys269 residue of PP2Ac in vitro

To identify the binding site of fostriecin on PP2Ac by covalent addition, native and fostriecin-treated PP2Ac was digested with trypsin and analyzed by MALDI-TOF MS analysis.[21,23,25] The human PP2A, consisting of a 36 kDa catalytic subunit (PP2Ac), a 55 kDa regulatory subunit (PP2Ab), and a 65 kDa structural subunit (PP2Aa), was treated with or without fostriecin (0.6 μM) for 2 h. The resulting PP2A was electrophoresed on 10% acrylamide gel, followed by band visualization with silver staining. Each band corresponding to PP2Ac was reduced with the addition of dithiothreitol and alkylated with acrylamide (71.0 Da), followed by in-gel digestion with trypsin and by MALDI-TOF MS analysis (Fig. 4A). The analysis of fostriecin-treated PP2Ac showed the presence of the fragment P-20 with a mass of 2069.9 Da (Fig. 4A (lower panel)), whereas this fragment was not observed in native PP2Ac (Fig. 4A (upper panel)).

The peptides derived from native PP2Ac after trypsin digestion were assigned from the theoretical molecular masses of the fragments in PP2Acα, one of the isomers of PP2Ac (Fig. 4B). Approximately 80% of the digested peptides, including nine cysteine-containing fragments, were identified (Table 1). Because the cysteine residues were alkylated with acrylamide (71.0 Da), the modification of one cysteine residue results in an additional mass of 71.0 Da. The calculated original (non-alkylated) masses of the nine cysteine (underlined)-containing fragments are as follows: 1478.8 (P-8, Q_{22}LSESQVKSL<u>C</u>EK_{34}), 1621.8 (P-10, <u>C</u>$_{269}$GNQAAI-MELDDTLK_{283}), 1646.8 (P-11, N_{255}VVTIFSAPNY<u>C</u>YR_{268}), 1647.8 (P-12, E_9LDQWIEQLNE<u>C</u>EK_{21}), 1734.8 (P-14, Q_{122}ITQVYGFYDE<u>C</u>LR_{135}), 1858.8 (P-15, A_{240}HQLVMEGYNW<u>C</u>HDR_{254}), 1862.9 (P-16, Q_{122}ITQ-VYGFYDE<u>C</u>LRK$_{136}$), 2452.1 (P-17, L_{186}QEVPHEGPM<u>C</u>DLLWSDPD-DR_{206}) and 2403.1 (P-18, <u>C</u>$_{50}$PVTV<u>C</u>GDVHGQFHDLMELEFR_{70}) Da. By comparing the original (non-alkylated) mass of P-10 with that of P-20, the difference of 448.1 Da between the mass of P-20 (2069.9 Da) and that of P-10 (1621.8 Da) possibly represented the molecular weight of hydrolyzed fostriecin (exact mass = 18.0 + 430.1 = 448.1). In our previous work, the lactone opening of PD 116,251, which is one of the members of the fostriecin family, occurred in H_2O at room temperature within 2 h (data

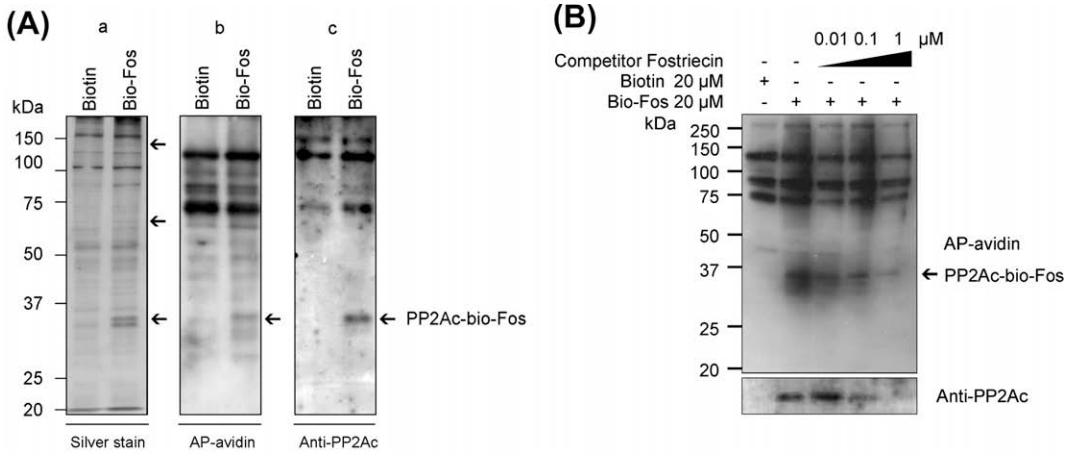

Figure 3. Fostriecin covalently binds to PP2Ac in HeLa S3 cells. (A) HeLa S3 cells were incubated with 20 μM bio-Fos or biotin for 2 h. After washing with phosphate buffered saline, the cells were lysed and bio-Fos- or biotin-binding proteins were recovered with streptavidin beads. After thorough washing of the beads, bound proteins were analyzed by sodium dodecyl sulfate polyacrylamide gel electrophoresis, followed by silver staining (a). Biotinylated proteins with bio-Fos or biotin were visualized by Western blot analysis using alkaline phosphatase-conjugated avidin (AP-avidin) (b). Proteins binding to bio-Fos or biotin were visualized by Western blot analysis using anti-PP2Ac antibody (c). (B) HeLa S3 cells were incubated in cell medium containing bio-Fos or biotin in the absence or presence of several concentrations of free fostriecin. After washing with phosphate buffered saline, the cells were lysed, and proteins bound to bio-Fos or biotin were recovered with streptavidin beads. Then, the beads were washed and bound proteins were analyzed by sodium dodecyl sulfate polyacrylamide gel electrophoresis, followed by visualization by Western blot analysis using AP-avidin or anti-PP2Ac antibody.

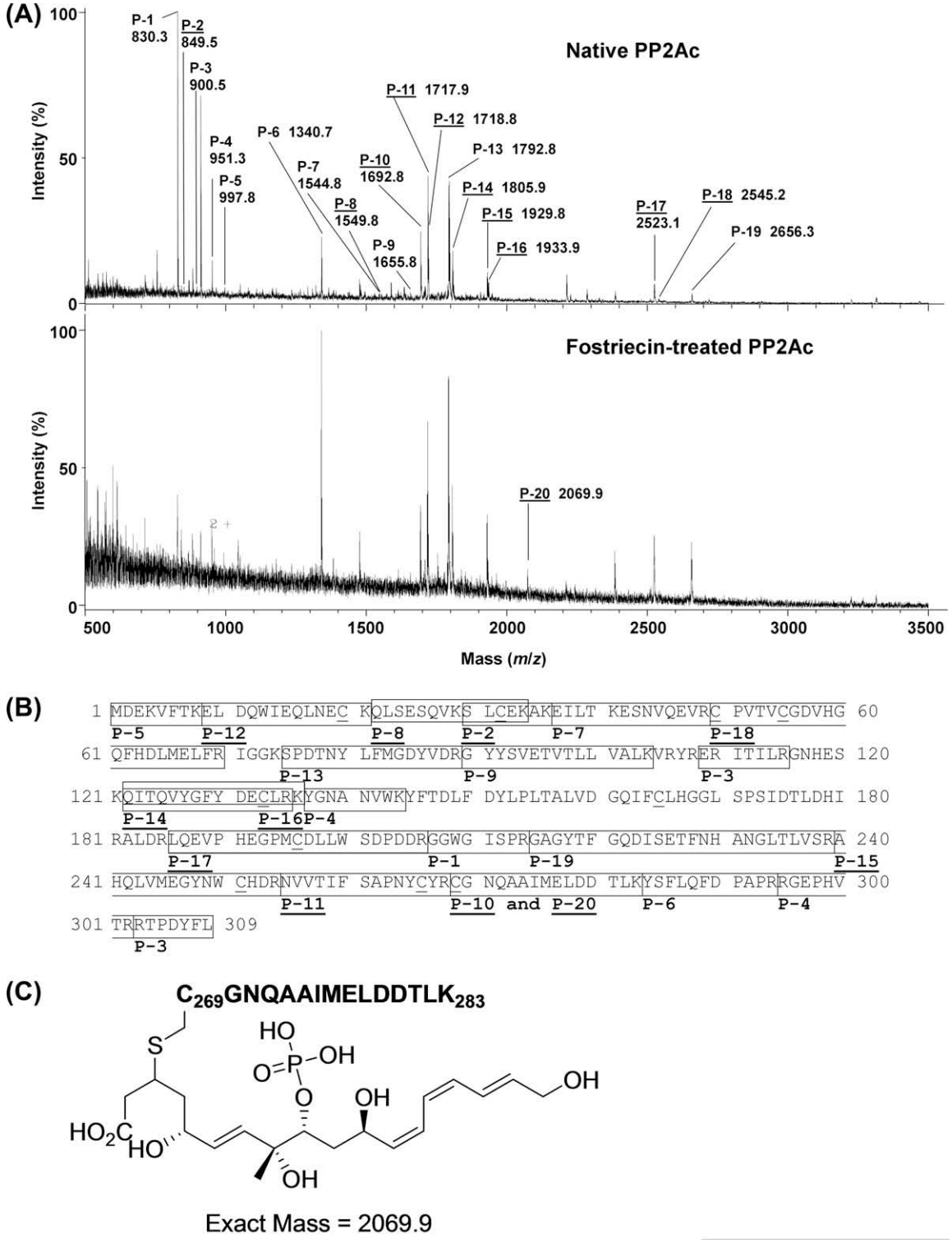

Figure 4. Matrix assisted laser desorption/ionization time-of-flight mass spectrometry (MALDI-TOF MS) analysis of native or fostriecin-treated PP2Ac digested with trypsin. (A) MALDI-TOF MS analysis of trypsin-digested PP2Ac. PP2A was incubated in the absence (upper panel) or presence (lower panel) of fostriecin (0.6 μM) at 30 °C for 2 h. After electrophoresis on 10% acrylamide gel, each band corresponding to PP2Ac was reduced with dithiothreitol and alkylated with acrylamide, followed by digestion with trypsin and analysis by MALDI-TOF MS. In the upper panel (fostriecin-untreated), the fragment with a mass of 1692.8 Da corresponds to Cys269-Lys283 conjugated with acrylamide. In the lower panel (fostriecin-treated), the fragment with a mass of 2069.9 Da was newly observed and this fragment corresponds to Cys269-Lys283 conjugated with the lactone-hydrolyzed fostriecin. (B) Tryptic digest fragments of native PP2Ac. The fragments were assigned by comparing the observed masses with those of the theoretical fragments. (C) Possible structure of fostriecin-modified Cys269-Lys283 fragment.

not shown). Hydrolysis of the lactone of phoslactomycin B, one of the members of the fostriecin family, under basic conditions has been reported by Reynolds and co-workers.[47] Taken together, these results suggest that the lactone opening of fostriecin occurs under the digesting process (Fig. 4C). MALDI post source decay MS/MS (MALDI-PSD-MS/MS) analysis of the fragments at m/z = 2069.9

Table 1
Peptides identified by MALDI-TOF MS from PP2Ac

Position	Peptide sequence	Calculated mass	MS	Peak
1–8	MDEKVFTK	997.5	997.8	P-5
9–21	ELDQWIEQLNECEK	1718.8	1718.8[a]	P-12
22–34	QLSESQVKSLCEK	1549.8	1549.8[a]	P-8
30–36	SLCEKAK	849.4	849.5	P-2
37–49	EILTKESNVQEVR	1544.8	1544.8	P-7
50–70	CPVTVCGDVHGQFHDLMELEFR	2545.2	2545.2[a]	P-18
75–89	SPDTNYLFMGDYVDR	1792.8	1792.8	P-13
90–104	GYYSVETVTLLVALK	1644.9	1655.8	P-9
109–115	ERITILR	900.6	900.5	P-3
122–135	QITQVYGFYDECLR	1805.9	1805.9[a]	P-14
122–136	QITQVYGFYDECLRK	1933.9	1933.9[a]	P-16
137–144	YGNANVWK	951.5	951.3	P-4
186–206	LQEVPHEGPMCDLLWSDPDDR	2523.1	2523.1[a]	P-17
207–214	GGWGISPR	829.4	830.3	P-1
215–239	GAGYTFGQDISETFNHANGLTLVSR	2655.3	2656.3	P-19
240–254	AHQLVMEGYNWCHDR	1929.8	1929.8[a]	P-15
255–268	NVVTIFSAPNYCYR	1717.8	1717.9[a]	P-11
269–283	CGNQAAIMELDDTLK	1692.8	1692.8[a]	P-10
269–283	(fostriecin-modified)CGNQAAIMELDDTLK	2069.9	2069.9	P-20
284–294	YSFLQFDPAPR	1340.6	1340.7	P-6
295–302	RGEPHVTR	951.3	951.5	P-4
303–309	RTPDYFL	911.5	911.3	P-3

[a] Acrylamide modification of cysteine results in a peptide mass increase of 71 Da per cysteine residue.

was performed to confirm the binding site of fostriecin. However, we obtained only the original fragment of peptides without fostriecin, suggesting that fostriecin moiety might be decomposed or removed by retro-Michael reaction under the MALDI-PSD-MS/MS conditions.

2.5. Fostriecin-binding model

After confirming the binding of fostriecin to the Cys269 residue of PP2Ac, we simulated a binding model of PP2Ac with fostriecin using the X-ray crystal structure of the PP2A core enzyme.[48] Because there are two cases in which the sulfhydryl group of the Cys269 residue in PP2Ac attacks from either *si*- or *re*-face at the C-3 position of fostriecin to provide (3*S*)- or (3*R*)-PP2Ac-conjugated fostriecin, respectively (Fig. 5A and B, respectively), we constructed two binding models, namely, (3*S*)- and (3*R*)-models, respectively (Fig. 5C and D, respectively). A 3D structure of fostriecin-conjugated PP2Ac was generated using energy minimization and molecular dynamics. The initial structure of PP2Ac with fostriecin was based on PP2Ac manually connected to fostriecin via *si*- or *re*-face at the C-3 position of fostriecin. The combined structure was optimized in vacuum using DISCOVERY STUDIO (DS) 2.0 program. The resulting (3*S*)- and (3*R*)-models are shown in Figure 5. In either case (Fig. 5E and F), fostriecin located over the active site of PP2Ac. In the (3*S*)-model (Fig. 5G), three amino acids in PP2Ac, namely, Ile123, Tyr127 and Gly215, formed a hydrophobic cage, including the hydrophobic triene moiety of fostriecin. On the other hand, in the (3*R*)-model (Fig. 5H), this hydrophobic cage was not buried. Multiple van der Waals interactions with the hydrophobic part of fostriecin appeared in either model (Fig. 5E–H) constructed with Tyr265, Arg268 and Leu243, and in the (3*S*)-model constructed with Gln242 and His241. The C9-phosphate esters of fostriecin interacted with the active site of manganese cations, and fostriecin blocked the paths toward these metal cations in either model.

3. Discussion

The inhibitory mechanism of fostriecin on PP2Ac has been identified in this study. This mechanism was previously suggested to be due to the covalent binding of fostriecin to the Cys269 residue of PP2Ac via the conjugate addition reaction of its α,β-unsaturated lactone. However, this conjugate addition has not yet been experimentally confirmed.[24,26,29]

In this study, we chemically synthesized bio-Fos in order to determine whether fostriecin covalently binds to PP2Ac. Because several antitumor natural products containing 4-substituted α,β-unsaturated lactone have been reported, such as phoslactomycin A,[49,50] kazusamycin A,[51] discodermolide[52,53] and pironetin A,[54,55] the introduction of biotin moiety at the C-4 position of fostriecin might not affect biological activity. The obtained bio-Fos was produced via a seven-step synthesis process with an overall yield of 22% from our previously synthesized compound (**12*Z***)-**7** (Scheme 1).[34] We found that bio-Fos shows cytotoxicity against the L1210 mouse leukemia cell line with an IC_{50} of 58 μM (Fig. 2). Although the cytotoxicity of bio-Fos was less than that of fostriecin (IC_{50} = 0.46 μM),[10] bio-Fos still retained cytotoxicity against L1210 and proved useful for PP2Ac isolation from living cells (Fig. 2).

We also demonstrated that PP2Ac directly bound to bio-Fos in HeLa S3 cells, and the resulting biotinylated PP2Ac was isolated from streptavidin-immobilized beads. In addition to PP2Ac, 65 and 130 kDa proteins were also isolated by immunoprecipitation using bio-Fos (Fig. 3A). We confirmed that PP2A covalently binds to bio-Fos by immunoblotting using alkaline phosphatase-conjugated avidin (Fig. 3B). However, the 65 and 130 kDa proteins were not detected by the immunoblotting, suggesting that these two proteins did not directly bind to bio-Fos. PP2A consists of PP2Ac, PP2Ab, and PP2Aa. Thus, the 65 kDa protein might be PP2Aa, which can be isolated from lysates as a complex with the PP2Ac-bio-Fos conjugate. Although the action of the 130 kDa protein remains unclear, both the 65 and 130 kDa proteins might interact with bio-Fos or PP2Ac by non-covalent binding.[12,15–17] Here, we confirmed that fostriecin binds to PP2Ac at the same binding site of bio-Fos since fostriecin competed with bio-Fos for binding to PP2Ac (Fig. 3).

The MALDI-TOF MS analysis demonstrating that fostriecin binds to the Cys269 residue (Fig. 4) strongly supports the result that the loop domain (260 F SAPNYCYRCG NQ 272) between the β12 (256 VVTI 259) and β13 (273 AAIMEL 278) loop serves as the critical region for PP2Ac inhibition by fostriecin.[28] This result also supports the finding that the PP2A C269S mutant in yeast is much less sensitive against fostriecin.[28] The fragment with a mass of 2069.9 Da

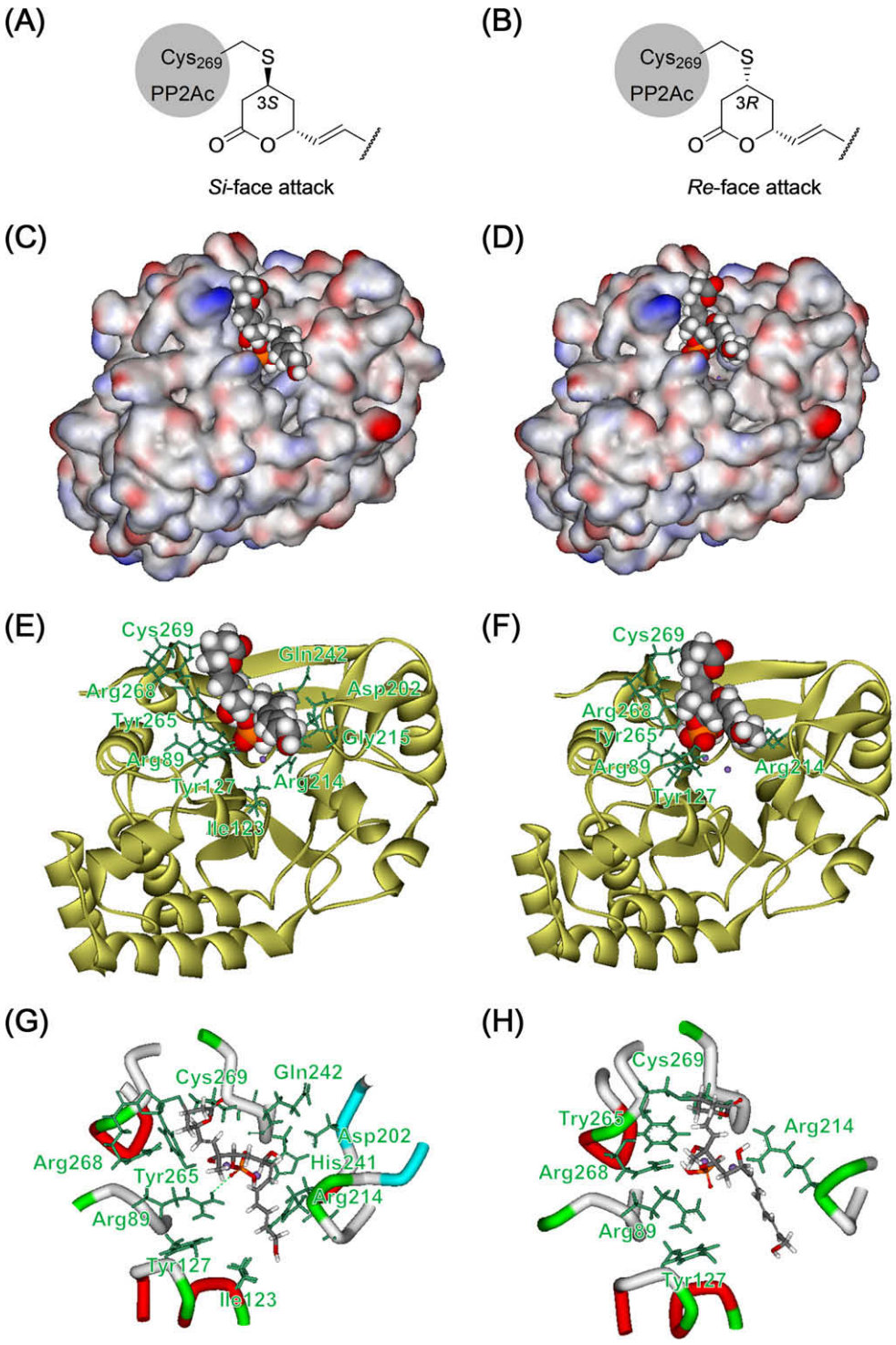

Figure 5. Proposed binding models of fostriecin–PP2Ac complex. (A and B) Structure of (3*S*)- (A) or (3*R*)-PP2Ac-conjugated fostriecin (B). (C–H) Docking model of PP2Ac with fostriecin, which was attacked from the *si*-face (C, E, G) or *re*-face (D, F, H) of fostriecin. Carbon, oxygen, hydrogen, nitrogen, sulfur and manganese are indicated in gray, red, white, blue, yellow and violet, respectively. PP2Ac residues near fostriecin are indicated in green. (C and D) Connolly surfaces and electronstatic potentials of fostriecin-conjugated PP2Ac. Blue denotes positive charge and red indicates negative charge. (E and F) Protein backbone (indicated in yellow) of fostriecin-conjugated PP2Ac. (G and H) Secondary structure of fostriecin-conjugated PP2Ac around fostriecin. The colors of the three-dimensional structure of the domain consisting of α-helix, β-sheet, turn, and flexible loop are red, blue, green and white, respectively.

corresponding to fostriecin-modified Cys269-Lys283 (269 C GNQAAIMELD DTLK 283) clearly appeared; however, the fragment with a mass of 1692.8 Da corresponding to Cys269-Lys283 did not completely disappear, suggesting that fostriecin might reversibly conjugate PP2Ac.

On the other hand, the peptide fragment conjugated with the lactone-opening derivative of fostriecin has been detected by MALDI-TOF MS analysis. However, we consider that hydrolysis of the lactone occurs during the tryptic digestion process, not within the cells. Furthermore, it is reported that fostriecin is unstable

and needs to be stored frozen in buffer.[2,8] Boger and co-workers reported that the lactone-opening derivative of fostriecin is less active against PP2A inhibition and loses cytotoxic activity.[27] Thus, we consider that fostriecin, occurring in the lactone-closed form, binds to PP2Ac and exerts inhibitory activity against this enzyme.

From these data, we constructed binding models of PP2Ac and conducted binding simulation of lactone-closed fostriecin with PP2Ac. Because of the two possibilities that the sulfhydryl group of the Cys269 residue of PP2Ac will bind to fostriecin via the *si*- or *re*-face of fostriecin to give (3*S*)- or (3*R*)-PP2Ac-conjugated fostriecin, respectively, we constructed two binding models of PP2Ac, namely, the (3*S*)- and (3*R*)-models, respectively (Fig. 5). In both models, the C9-phosphates bind or interact with the active site of manganese cations in PP2Ac, and conjugates fostriecin to prevent the substance of PP2Ac from entering the active site. This accounts for the decreased inhibitory activity of dephosphofostriecin (>10^5-fold) against PP2A.[27] The largest differences in the two models appeared in the surrounding area with the triene moiety of fostriecin. In the (3*S*)-model (Fig. 5E and G), the triene moiety of fostriecin is stabilized by a hydrophobic cage with Ile123, Tyr127 and Gly215.

4. Conclusion

Using an affinity matrix-based protein purification approach,[30–32] we directly demonstrated that fostriecin covalently binds to PP2Ac in HeLa S3 cells, specifically to the Cys269 residue of PP2Ac in vitro. The present findings may provide valuable information for the design and development of new biological tools and novel drugs for the treatment or prevention of cancer.

5. Experimental

5.1. Synthesis of biotin-labeled fostriecin (bio-Fos, 2)

5.1.1. General chemistry methods

^{1}H and ^{13}C NMR were recorded on a BRUKER DRX400 or DRX600. Chemical shifts were reported in δ, parts per million (ppm), relative to TMS as an internal standard or calibrated using residual undeuterated solvent as an internal reference. IR spectra were recorded on a JASCO FT/IR-410 spectrometer. Mass spectra were obtained on API QSTAR Pulsar i spectrometer. Optical rotations were measured on a JASCO P-1030 digital polarimeter. Column chromatography was carried out on Fuji Silisia PSQ100B. C18-reverse phase silica gel column chromatography was carried out on Fuji Silisia Chromatorex ODS (100–200 mesh). Analytical thin-layer chromatography (TLC) was performed on precoated Merck Silica Gel 60 F254 plates, and compounds were visualized by UV illumination (254 nm) or heating 150 °C after spraying phosphomolylbdic acid in ethanol. THF was distilled from sodium/benzophenone. CH_2Cl_2 was distilled from P_2O_5. All other solvent and reagents were obtained from commercial sources and used without further purification. Organic extracts were dried over Na_2SO_4, filtered, concentrated using a rotary evaporator. Involatile oils and solids were vacuum dried.

5.1.1.1. 2-[2-(Prop-2-yn-1-yloxy)ethoxy]ethyl 4-methylbenzene sulfonate (4). To a stirred solution of commercially available **3** (11.0 g, 76.3 mmol) in CH_2Cl_2 (150 mL) were added Et_3N (31.9 mL, 229 mmol) and DMAP (93 mg, 0.76 mmol) at 0 °C. The mixture was stirred for 15 min at the same temperature and a solution of TsCl (16.0 g, 83.9 mmol) in CH_2Cl_2 (150 mL) was added dropwise at the same temperature. The mixture was stirred at room temperature for 12 h. After the addition of saturated $NaHCO_3$ solution, the reaction mixture was extracted with EtOAc. The combined organic layers were washed with H_2O and saturated NaCl solution, dried over Na_2SO_4 and concentrated under reduced pressure. The resultant residue was purified by silica gel column chromatography (hexane/EtOAc = 4/1–1/1) to afford **4** as a colorless oil (20.1 g, 88%): IR, ^{13}C NMR and MS data were consistent with reported values.[56]

5.1.1.2. (4-{2-[2-(Prop-2-yn-1-yloxy)ethoxy]ethoxy}phenyl)methanol (5). To a stirred solution of **4** (111 mg, 0.35 mmol) in MeCN (0.7 mL) were added *p*-hydroxybenzylalcohol (30 mg, 0.24 mmol) and K_2CO_3 (48 mg, 0.35 mmol), and the mixture was refluxed overnight. After the addition of H_2O, the reaction mixture was extracted with EtOAc. The combined organic layers were washed with H_2O and saturated NaCl solution, dried over Na_2SO_4, and concentrated under reduced pressure. The resultant residue was purified by silica gel column chromatography (hexane/EtOAc = 2/1–1/1) to afford **5** as a white amorphous solid (56 mg, 64%): ^{1}H NMR (600 MHz, $CDCl_3$) δ 7.28 (2H, d, J = 8.5 Hz), 6.91 (2H, d, J = 8.5 Hz), 4.62 (2H, s), 4.21 (2H, d, J = 2.4 Hz), 4.14 (2H, t, J = 4.9 Hz), 3.86 (2H, t, J = 4.9 Hz), 3.72–3.77 (4H, m), 2.43 (1H, t, J = 2.4 Hz); ^{13}C NMR (100 MHz, $CDCl_3$) δ_C 158.3, 133.3, 128.5 (2C), 114.6 (2C), 79.5, 74.6, 70.6, 69.7, 69.0, 67.4, 64.9, 58.4; IR ν_{max} (neat) 3257, 2920, 2122, 1739, 1611, 1511 cm^{-1}; ESI-TOF HRMS m/z 273.1104 ($C_{14}H_{18}O_4$+Na$^+$ requires 273.1097).

5.1.1.3. (5*S*,6*S*)-6-[(1*E*,3*R*,4*R*,6*R*,7*Z*)-6-(*tert*-Butyldimethylsilyloxy)-8-iodo-3-methyl-3,4-bis(triethylsilyloxy)-octa-1,7-dien-1-yl]-5-hydroxy-5,6-dihydro-2*H*-pyran-2-one ((12*Z*)-7). (5*S*,6*S*)-6-[(1*E*,3*R*,4*R*,6*R*,7*EZ*)-6-(*tert*-Butyldimethylsilyloxy)-8-iodo-3-methyl-3,4-bis(triethylsilyloxy)-octa-1,7-dien-1-yl]-5-[(4-methoxybenzyl)oxy]-5,6-dihydro-2*H*-pyran-2-one (**12*EZ*)-7**[34] (*E*:*Z* = ca. 1:4) (801 mg, 0.92 mmol) was carefully purified by silica gel column chromatography (hexane/EtOAc = 9/1–6/1) to afford the (**12*Z*)-7** as a colorless oil (514 mg, 78%): $[\alpha]_D^{24}$ +70.3 (*c* 0.22, $CHCl_3$); ^{1}H NMR (600 MHz, $CDCl_3$) δ 6.99 (1H, dd, J = 9.7, 5.5 Hz), 6.21 (1H, d, J = 7.7 Hz), 6.18 (1H, dd, J = 7.7, 7.7 Hz), 6.14 (1H, d, J = 9.7 Hz), 6.08 (1H, dd, J = 15.9, 1.3 Hz), 5.68 (1H, dd, J = 15.9, 5.7 Hz), 4.94 (1H, ddd, J = 5.7, 2.8, 1.3 Hz), 4.43 (1H, ddd, J = 10.4, 7.7, 2.9 Hz), 4.13 (1H, dd, J = 5.5, 2.8 Hz), 3.76 (1H, dd, J = 8.2, 1.5 Hz), 2.31 (1H, br s, OH), 2.03 (1H, ddd, J = 13.9, 10.4, 1.5 Hz), 1.38 (3H, s), 1.13 (1H, ddd, J = 13.9, 8.2, 2.9 Hz), 1.00 (9H, t, J = 8.0 Hz), 0.96 (9H, t, J = 8.0 Hz), 0.88 (9H, s), 0.73 (6H, q, J = 8.0 Hz), 0.62 (6H, q, J = 8.0 Hz), 0.13 (3H, s), 0.06 (3H, s); ^{13}C NMR (100 MHz, $CDCl_3$) δ_C 163.1, 144.8, 144.1, 140.0, 123.1, 122.1, 80.0, 80.0, 77.5, 75.6, 72.9, 62.4, 40.7, 25.9 (3C), 21.0, 18.1, 7.3 (3C), 7.2 (3C), 6.7 (3C), 5.8 (3C), -3.0, -4.0; IR ν_{max} (neat) 3428, 2955, 2877, 1729, 1253 cm^{-1}; ESI-TOF HRMS m/z 775.2721 ($C_{32}H_{61}O_6Si_3I$+Na$^+$ requires 775.2712).

5.1.1.4. (5*S*,6*S*)-6-[(1*E*,3*R*,4*R*,6*R*,7*Z*)-6-(*tert*-Butyldimethylsilyloxy)-4-hydroxy-8-iodo-3-methyl-3-(triethylsilyloxy)-octa-1,7-dien-1-yl]-5-(4-{2-[2-(prop-2-yn-1-yloxy)ethoxy]ethoxy}benzyloxy)-5,6-di-hydro-2*H*-pyran-2-one (9). To a stirred solution of NaH (60%, 100 mg, 2.5 mmol) in CH_2Cl_2 (6 mL) was added **5** (2.5 g, 10.0 mmol), and the mixture was stirred for 30 min at room temperature. After the mixture was stirred for 15 min at 0 °C, a solution of Cl_3CCN (1.0 mL, 10.0 mmol) in CH_2Cl_2 (4 mL) was added dropwise at the same temperature, and the reaction mixture was stirred for 1 h at room temperature. After the addition of saturated $NaHCO_3$ solution, the reaction mixture was extracted with EtOAc. The combined organic layers were washed with H_2O and saturated NaCl solution, dried over Na_2SO_4, and concentrated under reduced pressure. The resultant imidate **6** as a violet oil was used directly to the next step without further purification.

To a stirred solution of (**12*Z*)-7** (45 mg, 0.060 mmol) and the crude **6** above (118 mg) in Et_2O (0.6 mL) was added $TrBF_4$

(0.6 mg, 1.8 μmol) at room temperature, and the mixture was stirred at the same temperature for 20 min. After the addition of $(HOCH_2CH_2)_2O$ (115 μl, 1.2 mmol) at the same temperature, the mixture was stirred at the same temperature for 10 min. Then saturated $NaHCO_3$ solution was added to the mixture. The reaction mixture was extracted with EtOAc and the combined organic layers were washed with H_2O and saturated NaCl solution. The resultant organic layer was dried over Na_2SO_4 and concentrated under reduced pressure. The resultant residue was roughly purified by silica gel column chromatography (hexane/EtOAc = 6/1–3/1) to provide the corresponding crude **8** as a colorless oil which was carried on directly to the next step without further purification.

To a stirred solution of the crude **8** above in MeCN (2.4 mL) and THF (1.2 mL) was added 1 M HCl aq (400 μL) at −10 °C, and the mixture has stirred at the same temperature for 2.5 h. After the addition of $NaHCO_3$ solution, the reaction mixture was extracted with EtOAc. The combined organic layers were washed with H_2O and saturated NaCl solution, dried over Na_2SO_4, and concentrated under reduced pressure. The resultant residue was purified by silica gel column chromatography (hexane/EtOAc = 4/1–2/1) to afford **9** as a colorless oil (36 mg, 69%): $[\alpha]_D^{24}$ +49.8 (*c* 0.13, $CHCl_3$); ^{1}H NMR (600 MHz, $CDCl_3$) δ 7.22 (2H, d, *J* = 8.6 Hz), 6.90 (2H, d, *J* = 8.6 Hz), 6.77 (1H, dd, *J* = 9.9, 4.3 Hz), 6.32 (1H, dd, *J* = 7.6, 7.6 Hz), 6.21 (1H, dd, *J* = 7.6, 0.9 Hz), 6.09 (1H, d, *J* = 9.9 Hz), 6.00 (1H, dd, *J* = 15.7, 4.3 Hz), 5.97 (1H, d, *J* = 15.7 Hz), 4.92 (1H, dd, *J* = 4.3, 4.3 Hz), 4.66 (1H, dddd, *J* = 7.6, 7.6, 3.0, 0.9 Hz), 4.57 (1H, d, *J* = 11.6 Hz), 4.51 (1H, d, *J* = 11.6 Hz), 4.22 (2H, d, *J* = 2.4 Hz), 4.14 (2H, t, *J* = 4.8 Hz), 4.08 (1H, t, *J* = 4.3 Hz), 3.87 (2H, t, *J* = 4.8 Hz), 3.73–3.78 (4H, m), 3.66 (1H, ddd, *J* = 10.8, 2.8, 1.2 Hz), 2.99 (1H, br d, *J* = 2.8 Hz, OH), 2.43 (1H, t, *J* = 2.4 Hz), 1.77 (1H, ddd, *J* = 14.0, 7.6, 1.2 Hz), 1.36 (1H, ddd, *J* = 14.0, 10.8, 3.0 Hz), 1.36 (3H, s), 0.94 (9H, t, *J* = 8.0 Hz), 0.88 (9H, s), 0.58 (6H, q, *J* = 8.0 Hz), 0.10 (3H, s), 0.06 (3H, s); ^{13}C NMR (100 MHz, $CDCl_3$)δ_C 162.8, 158.7, 144.0, 143.6, 139.5, 129.5, 129.3 (2C), 123.3, 122.8, 114.6 (2C), 80.0, 79.8, 79.5, 77.6, 74.8, 74.5, 74.1, 71.4, 70.6, 69.7, 69.1, 69.1, 67.4, 58.4, 37.0, 25.7 (3C), 22.8, 17.9, 7.1 (3C), 6.7 (3C), −4.5, −5.1; IR ν_{max} (neat) 3494, 3307, 2928, 1731, 1513 cm^{-1}; ESI-TOF HRMS *m/z* 893.2944 ($C_{40}H_{63}O_9Si_2I$+Na$^+$ requires 893.2947).

5.1.1.5. 2-(2-Azidoethoxy)ethanaminium chloride (11). To a stirred solution of **10** (11.7 g, 75 mmol) in EtOAc (600 mL) and 1 M HCl aq (120 mL) was added PPh_3 (20.6 g, 79 mmol) at room temperature, and the mixture was stirred for 4 h at the same temperature. After the addition of HCl (1 M in H_2O), the organic layer was extracted with H_2O. The combined aqueous layers were washed with EtOAc and concentrated under reduced pressure. The resultant residue was purified by C_{18}-reverse phase silica gel column chromatography (H_2O only to H_2O/MeOH = 1/1) to afford **11** as a white amorphous solid (9.9 g, 79%): ^{1}H NMR (600 MHz, D_2O) δ 3.66 (2H, t, *J* = 4.8 Hz), 3.61 (2H, t, *J* = 4.8 Hz), 3.40 (2H, t, *J* = 4.8 Hz), 3.09 (2H, t, *J* = 4.8 Hz); ^{13}C NMR (100 MHz, D_2O+MeOD) δ_C 70.5, 67.3, 51.62, 40.3; IR ν_{max} (film) 3114, 2113, 1625, 1407 cm^{-1}; ESI-TOF HRMS *m/z* 131.0927 ($C_4H_{10}N_4O$+H$^+$ requires 131.0927).

5.1.1.6. *N*-[2-(2-Azido-ethoxy)ethyl]-5-((3a*S*,4*S*,6a*R*)-2-oxohexahydro-1*H*-thieno[3,4-*d*]imidazol-4-yl)pentanamide (12). To a stirred solution of biotin (200 mg, 0.82 mmol), **11** (264 mg, 1.6 mmol) and *i*-Pr_2NEt (820 μl, 4.8 mmol) in DMF (6.5 mL) was added HBTU (308 mg, 0.81 mmol) at room temperature, and the mixture was stirred overnight at the same temperature. After the addition of saturated $NaHCO_3$ solution, the reaction mixture was extracted with EtOAc. The combined organic layers were washed with H_2O and saturated NaCl solution, dried over Na_2SO_4, and concentrated under reduced pressure. The resultant residue was purified by C_{18}-reverse phase silica gel column chromatography (H_2O/MeOH = 3/1–1/1) to afford **12** as a white amorphous solid (252 mg, 89%): $[\alpha]_D^{24}$ +49.4 (*c* 0.93, H_2O); ^{1}H NMR (600 MHz, D_2O) δ 4.43 (1H, dd, *J* = 7.9, 5.0 Hz), 4.25 (1H, dd, *J* = 7.9, 4.6 Hz), 3.54 (2H, t, *J* = 4.9 Hz), 3.48 (2H, t, *J* = 5.3 Hz), 3.31 (2H, t, *J* = 4.9 Hz), 3.23 (2H, t, *J* = 5.3 Hz), 3.20 (1H, ddd, *J* = 9.8, 4.6, 4.6 Hz), 2.82 (1H, dd, *J* = 13.1, 5.0 Hz), 2.61 (1H, d, *J* = 13.1 Hz), 2.11 (2H, t, *J* = 7.3 Hz), 1.38–1.59 (4H, m), 1.29–1.24 (2H, m); ^{13}C NMR (100 MHz, MeOD) δ_C 176.9, 166.1, 70.6, 70.1, 63.2, 61.4, 56.7, 51.5, 40.9, 40.1, 36.7, 29.4, 29.2, 26.5; IR ν_{max} (KBr) 3288, 2925, 2105, 1696, 1551 cm^{-1}; ESI-TOF HRMS *m/z* 379.1531 ($C_{14}H_{24}N_6O_3S$+Na$^+$ requires 379.1522).

5.1.1.7. *N*-{2-[2-(4-{[2-(2-{4-[({(2*S*,3*S*)-2-[(1*E*,3*R*,4*R*,6*R*,7*Z*)-6-(*tert*-Butyldimethylsilyloxy)-4-hydroxy-8-iodo-3-methyl-3-(triethylsilyloxy)-octa-1,7-dien-1-yl]-6-oxo-3,6-dihydro-2*H*-pyran-3-yl}oxy)methyl]phenoxy}ethoxy)ethoxy]methyl}-1*H*-1,2,3-tri-azol-1-yl)ethoxy]ethyl}-5-((3a*S*,4*S*,6a*R*)-2-oxohexahydro-1*H*-thieno[3,4-*d*]imidazol-4-yl)pentanamide (14). To a stirred solution of **9** (66 mg, 0.075 mmol), **12** (108 mg, 0.3 mmol) and Et_3N (315 μL, 2.3 mmol) in THF (8 mL) was added CuI(I) (144 mg, 0.75 mmol) at room temperature. The mixture was stirred at the same temperature for 1 h, then **12** (108 mg, 0.3 mmol) was added, and stirred for 20 min at the same temperature. After the addition of saturated NH_4Cl solution (1 mL), H_2O (4 mL) and MeOH (1 mL) in this order, the reaction mixture was purified directly by C_{18}-reverse phase silica gel column chromatography (H_2O only to MeOH only) to afford **14** as a colorless oil (91 mg, 98%): $[\alpha]_D^{24}$ +71.0 (*c* 0.75, $CHCl_3$); ^{1}H NMR (600 MHz, MeOD) δ 7.97 (1H, s), 7.24 (2H, d, *J* = 8.6 Hz), 7.02 (1H, dd, *J* = 9.9, 4.9 Hz), 6.91 (2H, d, *J* = 8.6 Hz), 6.22 (1H, d, *J* = 7.6 Hz), 6.15 (1H, dd, *J* = 7.6, 7.6 Hz), 6.08 (1H, d, *J* = 9.9 Hz), 6.05 (1H, d, *J* = 15.7, 4.0 Hz), 6.02 (1H, dd, *J* = 15.7, 2.3 Hz), 5.00 (1H, ddd, *J* = 4.0, 3.6, 2.3 Hz), 4.64 (2H, s), 4.64 (1H, ddd, *J* = 9.5, 7.6, 2.9 Hz), 4.53–4.56 (4H, m), 4.46 (1H, dd, *J* = 7.8, 4.8 Hz), 4.26 (1H, dd, *J* = 7.8, 4.6 Hz), 4.10–4.13 (2H, m), 4.08 (1H, dd, *J* = 4.9, 3.6 Hz), 3.81–3.85 (4H, m), 3.68–3.74 (4H, m), 3.66 (1H, dd, *J* = 10.7, 1.2 Hz), 3.49 (2H, t, *J* = 5.4 Hz), 3.29–3.32 (2H, m), 3.16 (1H, ddd, *J* = 9.1, 5.6, 4.6 Hz), 2.89 (1H, dd, *J* = 12.8, 4.8 Hz), 2.68 (1H, d, *J* = 12.8 Hz), 2.18 (2H, t, *J* = 7.4 Hz), 1.89 (1H, ddd, *J* = 13.8, 9.5, 1.2 Hz), 1.52–1.74 (4H, m), 1.38–1.43 (2H, m), 1.28 (3H, s), 1.23 (1H, ddd, *J* = 13.8, 10.7, 2.9 Hz), 0.97 (9H, t, *J* = 7.9 Hz), 0.89 (9H, s), 0.64 (6H, q, *J* = 7.9 Hz), 0.13 (3H, s), 0.06 (3H, s); ^{13}C NMR (100 MHz, MeOD) δ_C 176.1, 166.1, 165.6, 160.2, 146.1, 146.1, 145.9, 140.4, 131.4, 130.6 (2C), 125.8, 124.8, 123.5, 115.6 (2C), 82.1, 80.0, 78.8, 75.6, 74.3, 72.9, 71.8, 70.9, 70.9, 70.7, 70.5, 70.1, 68.7, 65.1, 63.4, 61.6, 57.0, 51.4, 41.0, 40.2, 39.4, 36.7, 29.8, 29.5, 26.8, 26.5 (3C), 25.6, 19.0, 7.9 (3C), 7.7 (3C), −3.8, −4.4; IR ν_{max} (neat) 3299, 2927, 2108, 1698, 1252 cm^{-1}; ESI-TOF HRMS *m/z* 1249.4571 ($C_{54}H_{87}N_6O1_2Si_2SI$+Na$^+$ requires 1249.4578).

5.1.1.8. *N*-{2-[2-(4-{[2-(2-{4-[({(2*S*,3*S*)-2-[(1*E*,3*R*,4*R*,6*R*,7*Z*,9*Z*,-11*E*)-6-(*tert*-Butyldimethylsilyloxy)-13-(*tert*-butyldiphenylsilyloxy)-4-hydroxy-3-methyl-3-(triethylsilyloxy)-trideca-1,7,9,11-tetraen-1-yl]-6-oxo-3,6-dihydro-2*H*-pyran-3-yl}oxy)methyl]phenoxy}ethoxy)ethoxy]methyl}-1*H*-1,2,3-triazol-1-yl)ethoxy]ethyl}-5-((3a*S*,4*S*,6a*R*)-2-oxohexahydro-1*H*-thieno[3,4-*d*]imidazol-4-yl) pentanamide (15). To a stirred solution of stannane **13**[41,42] (29 mg, 0.047 mmol) and **14** (9.6 mg, 7.8 μmol) in DMF (500 μl) was added $Pd(MeCN)_2Cl_2$ (0.2 mg, 0.77 μmol) at 0 °C. The resultant mixture was stirred at the same temperature for 10 h. After the addition of saturated $NaHCO_3$ solution, the reaction mixture was extracted with $CHCl_3$. The combined organic layers were washed with H_2O and saturated NaCl solution, dried over Na_2SO_4 and concentrated under reduced pressure. The resultant residue was directly purified by silica gel column chromatography ($CHCl_3$ only to $CHCl_3$/MeOH = 4/1) to afford **15** as a colorless oil (9.0 mg, 81%): $[\alpha]_D^{24}$ +21.5 (*c* 0.35, $CHCl_3$); ^{1}H NMR (600 MHz, $CDCl_3$) δ 7.66–7.70

(5H, m), 7.35–7.44 (6H, m), 7.22 (2H, d, J = 8.7 Hz), 6.89 (2H, d, J = 8.7 Hz), 6.77 (1H, dd, J = 9.9, 4.5 Hz), 6.74 (1H, ddd, J = 15.0, 11.3, 1.0 Hz), 6.33 (1H, dd, J = 11.3, 11.3 Hz), 6.19 (1H, t, J = 4.9 Hz, NH), 6.14 (1H, dd, J = 11.3, 11.3 Hz), 6.08 (1H, dd, J = 9.9, 0.6 Hz), 6.04 (1H, dd, J = 11.3, 11.3 Hz), 5.99 (1H, dd, J = 16.4, 3.8 Hz), 5.95 (1H, dd, J = 16.4, 2.1 Hz), 5.83 (1H, dt, J = 15.0, 4.5 Hz), 5.62 (1H, br s, NH), 5.53 (1H, dd, J = 11.3, 8.4 Hz), 4.89–4.94 (2H, m), 4.76 (1H, br s, NH), 4.71 (2H, s), 4.57 (1H, d, J = 11.7 Hz), 4.51 (2H, t, J = 5.0 Hz), 4.50 (1H, d, J = 11.7 Hz), 4.48 (1H, dd, J = 7.3, 5.3 Hz), 4.31 (1H, dt, J = 7.3, 4.9 Hz), 4.29 (2H, dd, J = 4.5, 1.0 Hz), 4.12 (2H, t, J = 4.8 Hz), 4.08 (1H, ddd, J = 4.5, 3.9, 0.6 Hz), 3.83–3.86 (4H, m), 3.73–7.76 (4H, m), 3.70 (1H, br dd, J = 11.5, 2.7 Hz), 3.52 (2H, t, J = 4.9 Hz), 3.38 (2H, dt, J = 4.9, 4.9 Hz), 3.14, (1H, td, J = 7.3, 4.9 Hz), 2.99 (1H, br d, J = 2.7 Hz, OH), 2.90 (1H, dd, J = 12.4, 5.3 Hz), 2.70 (1H, d, J = 12.4 Hz), 2.20 (2H, t, J = 7.1 Hz), 1.67–1.76 (1H, m), 1.57–1.76 (4H, m), 1.40–1.47 (2H, m), 1.33–1.40 (1H, m), 1.34 (3H, s), 1.08 (9H, s), 0.92 (9H, t, J = 7.9 Hz), 0.88 (9H, s), 0.57 (6H, q, J = 7.9 Hz), 0.06 (3H, s), 0.03 (3H, s); ^{13}C NMR (100 MHz, $CDCl_3$) δ_C 173.1, 163.0, 162.9, 158.7, 145.1, 143.7, 139.7, 135.6, 135.5 (4C), 134.3, 133.6, 133.5, 130.0, 129.7, 129.7 (2C), 129.4 (2C), 127.7 (4C), 124.5, 123.7, 123.3, 123.2, 122.8, 122.2, 114.6 (2C), 80.1, 77.7, 74.9, 71.5, 70.8, 69.8, 69.7, 69.7, 69.2, 68.8, 67.5, 67.0, 64.7, 64.2, 61.8, 60.0, 55.4, 50.1, 40.6, 39.0, 38.9, 35.6, 28.0, 27.9, 26.8 (3C), 25.8 (3C), 25.4, 22.6, 19.2, 18.1, 7.1 (3C), 6.7 (3C), −4.3, −5.0; IR ν_{max} (neat) 3299, 2927, 2108, 1698, 1252 cm^{-1}; ESI-TOF HRMS m/z 1443.7170 ($C_{75}H_{112}N_6O_{13}Si_3S$+Na$^+$ requires 1443.7208).

5.1.1.9. *N,N*-Diethylethanaminium (1*E*,3*R*,4*R*,6*R*,7*Z*,9*Z*,11*E*)-3,6, 13-trihydroxy-1-{(2*S*,3*S*)-3-[(4-{2-[2-({1-[2-(2-{[5-((3a*S*,4*S*,6a*R*)-2-oxohexahydro-1*H*-thieno[3,4-*d*]imidazol-4-yl)pentanoyl] amino} ethoxy)ethyl]-1*H*-1,2,3-triazol-4-yl}methoxy)ethoxy] ethoxy} benzyl)oxy]-6-oxo-3,6-dihydro-2*H*-pyran-2-yl}-3-methyl-trideca -1, 7,9,11-tetraen-4-yl hydrogen phosphate (2). To a stirred solution of **15** (7.6 mg, 5.3 μmol) and tetrazole (5.6 mg, 0.080 mmol) in CH_2Cl_2 (500 μL) was added *i*-$Pr_2NP(OFm)_2$[43,44] (28 mg, 0.053 mmol) at room temperature, and the mixture was stirred at the same temperature for 20 min. After the addition of TBHP (3.2 M in CH_2Cl_2, 60 μL, 0.96 mmol) at 0 °C, the resulting mixture was stirred at the same temperature for 1 h. Following addition of MeOH (0.2 mL) and $CHCl_3$ (0.5 mL), the reaction mixture was directly roughly purified by silica gel column chromatography ($CHCl_3$ only to $CHCl_3$/MeOH = 9/1) to give roughly purified **16**, which was used directly to the next step.

To a stirred solution of crude **16** above in MeCN (0.5 mL) was added Et_3N (0.1 mL, 0.71 mmol) at 0 °C, and the mixture was stirred at room temperature for 17 h. The mixture was concentrated under reduced pressure to give crude phosphate monoester **17**, which was used directly to the next step.

The reaction was performed in a plastic vessel. To a stirred solution of the crude phosphate monoester **17** above in MeCN (0.5 mL) were added $Et_3N{\cdot}3HF$ (26 μL, 0.16 mmol) and Et_3N (11 μL, 0.079 mmol) at 60 °C, and the mixture was stirred at the same temperature for 2 h. After the addition of 0.5 M $NaHCO_3$ aq (1.9 mL, 0.95 mmol) at 0 °C and H_2O (720 μL), the reaction mixture was directly purified by C_{18}-reverse phase silica gel column chromatography (H_2O only to H_2O/MeCN = 9/1) to afford **2** as white crystals (2.2 mg, 37%): $[\alpha]_D^{24}$ +43.2 (*c* 0.08, MeOH); ^{1}H NMR (MeOD, 600 MHz) δ 7.96 (1H, s), 7.27 (2H, d, J = 8.6 Hz), 6.99 (1H, dd, J = 9.8, 5.1 Hz), 6.91 (2H, d, J = 8.6 Hz), 6.73 (1H, dd, J = 15.0, 12.2 Hz), 6.43 (1H, dd, J = 11.6, 11.6 Hz), 6.37 (1H, dd, J = 11.6, 11.6 Hz), 5.99–6.11 (4H, m), 5.84 (1H, dt, J = 15.0, 5.7 Hz), 5.48 (1H, dd, J = 11.6, 9.8 Hz), 5.02 (1H, dd, J = 9.8, 9.8 Hz), 4.99 (1H, dd, J = 6.6, 3.2 Hz), 4.64 (2H, s), 4.49–4.58 (4H, m), 4.56 (1H, dd, J = 7.7, 5.0 Hz), 4.30 (1H, ddd, J = 11.3, 11.3, 1.8 Hz), 4.26 (1H, dd, J = 7.7, 4.7 Hz), 4.10–4.14 (4H, m), 4.08 (1H, dd, J = 5.1, 3.2 Hz), 3.80–3.84 (4H, m), 3.68–3.73 (4H, m), 3.48 (2H, t, J = 5.4 Hz), 3.25–3.33 (2H, m), 3.15 (1H, dt, J = 10.1, 4.7 Hz), 3.12 (6H, q, J = 10.9 Hz, Et_3N), 2.89 (1H, dd, J = 12.8, 5.0 Hz), 2.68 (1H, d, J = 12.8 Hz), 2.18 (2H, t, J = 7.4 Hz), 1.52–1.74 (4H, m), 1.60–1.70 (1H, m), 1.42–1.51 (1H, m), 1.29–1.42 (2H, m), 1.35 (3H, s), 1.27 (9H, t, J = 10.9 Hz, Et_3N); ^{13}C NMR (100 Hz, MeOD) δ_C 176.2, 166.1, 165.7, 160.2, 146.1, 145.9, 140.8, 135.9, 135.6, 131.5, 130.9 (2C), 130.8, 126.6, 125.8, 125.3, 124.5, 124.2, 123.2, 115.6 (2C), 82.3, 79.2 (J_{C-P} = 7 Hz), 75.7 (J_{C-P} = 1.7 Hz), 73.3, 71.8, 70.9, 70.9, 70.6, 70.5, 70.1, 68.7, 65.1, 64.6, 63.4, 63.3, 61.6, 57.0, 51.4, 47.0 (3C, Et_3N), 41.1, 40.9 (J_{C-P} = 1.4 Hz), 40.2, 36.7, 29.8, 29.5, 26.8, 24.6, 9.24 (3C, Et_3N); ^{31}P NMR(162 MHz, MeOD) δ_P 3.6; IR ν_{max} (KBr) 3429, 2925, 1697, 1514, 1458 cm^{-1}; ESI-TOF HRMS m/z 1136.5335 ($C_{53}H_{82}N_7O_{16}PS$+H$^+$ requires 1136.5349).

5.2. Cell culture

Murine leukemia L1210 cells (provided by Cell Resource Center for Biomedical Research, Tohoku University) were cultured in RPMI 1640 medium (Nacalai Tesque) with 10% fetal calf serum (TRACE SCIENTIFIC LTD.), 2 mM L-glutamine, penicillin (100 units/mL), and streptomycin (100 μg/mL) at 37 °C in 5% CO_2.

5.3. Growth inhibition assay

Cell proliferation was evaluated using Cell Count Reagent SF (Nacalai Tesque). Cells are inoculated into 96-well plates containing 5000 cells in total volume of 100 μL in each well. After the incubation with bio-Fos (0, 5, 10, 25, 50, 100, 250, 500 and 1000 μM) for 72 h, 10 μl of Cell Count Reagent was added to each well 2 h before evaluating cell proliferation on ARVO SX microplate reader (WALLAC) at 450 nm. Each experimental condition was assayed in tetralicate, and all experiments were performed at least three times. Percentage growth inhibition is calculated from time zero, control growth, and the each concentration level of absorbance.

5.4. In situ fostriecin-binding assay

Full confluent HeLa S3 cells (ca. 1 g of wet weight) adherent to wells were incubated in medium (see above) containing 20 μM of bio-Fos or biotin at 37 °C for 2 h. After the wash of the cells with phosphate buffered saline (PBS) (H_3PO_4 137 mM NaCl, 118 mM [pH 7.4]) three times, cells were scraped from the wells in PBS, followed by transferring the cells to a clean Eppendorf tube, centrifugation at 350*g* and discard of the supernatant. The cells were treated with 100 μL of the lysis buffer (50 mM Tris–HCl, 150 mM NaCl, 1 mM EDTA, 2.5 mM EGTA, 0.1% NP-40, 0.1 mM PMSF, 1% Protease Inhibitor Cocktail (EDTA free) (nacalai tesque) [pH 7.5]) and placed on ice for 1 h. After centrifugation at 16,000*g*, streptavidin–agarose (20 μL, Aldrich) were added to supernatant of the lysate, followed by the mixing with rotator at 4 °C for 30 min. Then the beads, together with bound proteins, were washed with 1 ml of beads-washing buffer (25 mM Tris–HCl, 137 mM NaCl, 0.05% Tween 20 [pH 7.5]) 10 times and boiled in 20 μl of SDS-loading buffer (50 mM Tris–HCl, 10% glycerol, 2.0% SDS, 5% 2-mercaptoethanol, and a few drops of bromophenol blue [pH 6.8]). The resultant mixtures were electrophoresed on 10% acrylamide gels, followed by analyze by silver stain or western blotting using an alkaline phosphatase-conjugated avidin (1:500 dilution, Zymed) or anti-PP2Ac antibody (1:500 dilution, rabit polyclonal, Calbiochem). The alkaline phosphatase-conjugated anti-rabit IgG (1:2000 dilution, Sigma) was used as secondary antibody. The protein bands were visualized by the use of CDP-Star (GE Healthcare Bio-Sciences).

5.5. Determination of the fostriecin binding site by mass spectrometry

To the solution of fostriecin (0.5 mM in H_2O, 2 μL, 1 nmol) or H_2O (2 μl) in 13 μL of tris–HCl buffer (25 mM Tris–HCl, 137 mM NaCl [pH 7.5]) was added 5 μl of PP2A (0.5 unit, Upstate). After the incubation of the mixtures at 30 °C for 2 h, 6 μl of 5× SDS-loading buffer (250 mM Tris–HCl, 50% glycerol, 10% SDS, 25% 2-mercaptoethanol, and a few drops of bromophenol blue [pH 6.8]), H_2O (2.5 μL) and dithiothreitol (1 M in H_2O, 1.5 μL) were added, followed by boiling for 1 min. The resulting samples were electrophoresed on 10% acrylamide gels, followed by the reduction with dithiothreitol and the alkylation with acrylamide. After the digestion with trypsin (Promega) at 37 °C for 16 h, the resulting peptides (0.5 μL) were spotted onto the MALDI target with a MALDI matrix solution (2.5-dihydroxybenzoic acid), followed by co-crystallization of the sample and matrix at room temperature. The molecular weights of the generated peptides were determined by a reflex IV MALDI-TOF mass spectrometer (Bruker Daltonics, Billerica, MA, USA).

5.6. Protein-inhibitor docking modeling

The generation of docking models was performed using a fixed docking procedure in the Minimization and Dynamics protocols within DISCOVERY STUDIO (DS) 2.0 modeling software (Accerlys Inc., San Diego, CA, USA). The calculations used a CHARMm force-field. All calculations were conducted on an IBM Blade Center (312 processors and 624 GB of memory). The PP2Ac (PDB entry: 2IE4)[48] was refined based on molecular dynamic simulations using standard dynamics cascade protocol in DS. The fostriecin–PP2Ac model was constructed with the Minimization and Dynamics protocols within DS 2.0.

Acknowledgments

We thank Cell Resource Center for Biomedical Research, Institute of Development, Aging and Cancer, Tohoku University, for providing HeLa S3 cells.

Supplementary data

Supplementary data associated with this article can be found, in the online version, at doi:10.1016/j.bmc.2009.09.050.

References and notes

1. Tunac, J. B.; Graham, B. D.; Dobson, W. E. *J. Antibiot.* **1983**, *36*, 1595.
2. Stampwala, S. S.; Bunge, R. H.; Hurley, T. R.; Willmer, N. E.; Brankiewicz, A. J.; Steinman, C. E.; Smitka, T. A.; French, J. C. *J. Antibiot.* **1983**, *36*, 1601.
3. Hokanson, G. C.; French, J. C. *J. Org. Chem.* **1985**, *50*, 462.
4. Stampwala, S. S.; French, J. C.; Tunac, J. B.; Hurley, T. R.; Bunge, R. H. European Patent Appl. 87021 A2, 1983.
5. Stampwala, S. S.; French, J. C.; Tunac, J. B.; Hurley, T. R.; Bunge, R. H. U.S. Patent 447, 544, 1986.
6. Lewy, D. S.; Gauss, C.-M.; Soenen, D. R.; Boger, D. L. *Curr. Med. Chem.* **2002**, *9*, 2005.
7. Jackson, R. C.; Fry, D. W.; Boritzki, T. J.; Roberts, B. J.; Hook, K. E.; Leopold, W. R. *Adv. Enzyme Regul.* **1985**, *23*, 193.
8. de Jong, R. S.; de Vries, E. G. E.; Mulder, N. H. *Anticancer Drugs* **1997**, *8*, 413.
9. Scheithauer, W.; von Hoff, D. D.; Clark, G. M.; Shillis, J. L.; Elslager, E. F. *Eur. J. Cancer Clin. Oncol.* **1986**, *22*, 921.
10. Leopold, W. R.; Shillis, J. L.; Mertus, A. E.; Nelson, J. M.; Roberts, B. J.; Jackson, R. C. *Cancer Res.* **1984**, *44*, 1928.
11. Boritzki, T. J.; Wolfard, T. S.; Besserer, J. A.; Jackson, R. C.; Fry, D. W. *Biochem. Pharmacol.* **1988**, *37*, 4063.
12. Roberge, M.; Tudan, C.; Hung, S. M. F.; Harder, K. W.; Jirik, F. R.; Anderson, H. *Cancer Res.* **1994**, *54*, 6115.
13. Guo, X. W.; Th'ng, J. P.; Swank, R. A.; Anderson, H. J.; Tudan, C.; Bradbury, E. M.; Roberge, M. *EMBO J.* **1995**, *14*, 976.
14. Ho, D. T.; Roberge, M. *Carcinogenesis* **1996**, *17*, 967.
15. Walsh, A. H.; Cheng, A.; Honkanen, R. E. *FEBS Lett.* **1997**, *416*, 230.
16. Hastie, C. J.; Cohen, P. T. *FEBS Lett.* **1998**, *431*, 357.
17. Cheng, A.; Balczon, R.; Zuo, Z.; Koons, J. S.; Walsh, A. H.; Honkanen, R. E. *Cancer Res.* **1998**, *58*, 3611.
18. Chiang, C.-W.; Harris, G.; Ellig, C.; Masters, S. C.; Subramanian, R.; Shenolikar, S.; Wadzinski, B. E.; Yang, E. *Blood* **2001**, *97*, 1289.
19. Douglas, P.; Moorhead, G. B. G.; Ye, R.; Lees-Miller, S. P. *J. Biol. Chem.* **2001**, *276*, 18992.
20. Rossi, A.; Kapahi, P.; Natoli, G.; Takahashi, T.; Chen, Y.; Karin, M.; Santoro, M. G. *Nature* **2000**, *403*, 103.
21. Kudo, N.; Matsumori, N.; Taoka, H.; Fujiwara, D.; Schreiner, E. P.; Wolff, B.; Yoshida, M.; Horinouchi, S. *Proc. Natl. Acad. Sci. U.S.A.* **1999**, *96*, 9112.
22. Usui, T.; Watanabe, H.; Nakayama, H.; Tada, Y.; Kanoh, N.; Kondoh, M.; Asao, T.; Takio, K.; Watanabe, H.; Nishikawa, K.; Kitahara, T.; Osada, H. *Chem. Biol.* **2004**, *11*, 799.
23. Usui, T.; Kazami, S.; Dohmae, N.; Mashimo, Y.; Kondo, H.; Tsuda, M.; Terasaki, A. G.; Ohashi, K.; Kobayashi, J.; Osada, H. *Chem. Biol.* **2004**, *11*, 1269.
24. Teruya, T.; Simizu, S.; Kanoh, N.; Osada, H. *FEBS Lett.* **2005**, *579*, 2463.
25. Takeuchi, T.; Ishidoh, T.; Iijima, H.; Kuriyama, I.; Shimazaki, N.; Koiwai, O.; Kuramochi, K.; Kobayashi, S.; Sugawara, F.; Sakaguchi, K.; Yoshida, H.; Mizushina, Y. *Genes cells* **2006**, *11*, 223.
26. Lawhorn, B. G.; Boga, S. B.; Wolkenberg, S. E.; Colby, D. A.; Gauss, C.-M.; Swingle, M. R.; Amable, L.; Honkanen, R. E.; Boger, D. L. *J. Am. Chem. Soc.* **2006**, *128*, 16720.
27. Buck, S. B.; Hardouin, C.; Ichikawa, S.; Soenen, D. R.; Gauss, C.-M.; Hwang, I.; Swingle, M. R.; Bonness, K. M.; Honkanen, R. E.; Boger, D. L. *J. Am. Chem. Soc.* **2003**, *125*, 15694.
28. Evans, D. R. H.; Simon, J. A. *FEBS Lett.* **2001**, *498*, 110.
29. Swingle, M. R.; Amable, L.; Lawhorn, B. G.; Buck, S. B.; Burke, C. P.; Ratti, P.; Fischer, K. L.; Boger, D. L.; Honkanen, R. E. *J. Pharmacol. Exp. Ther.* **2009**, *331*, 45.
30. Lefkowitz, R. J.; Haber, E.; O'Hara, D. *Proc. Natl. Acad. Sci. U.S.A.* **1972**, *69*, 2828.
31. Harding, M. W.; Galat, A.; Uehling, D. E.; Schreiber, S. L. *Nature* **1989**, *341*, 758.
32. Khersonsky, S. M.; Jung, D.-W.; Kang, T.-W.; Walsh, D. P.; Moon, H.-S.; Jo, H.; Jacobson, E. M.; Shetty, V.; Neubert, T. A.; Chang, Y.-T. *J. Am. Chem. Soc.* **2003**, *125*, 11804.
33. Sin, N.; Meng, L.; Wang, M. Q. W.; Wen, J. J.; Bornmann, W. G.; Crews, C. M. *Proc. Natl. Acad. Sci. U.S.A.* **1997**, *94*, 6099.
34. Takeuchi, T.; Kuramochi, K.; Kobayashi, S.; Sugawara, F. *Org. Lett.* **2006**, *8*, 5307. Additions and corrections of this paper. ibid. **2007**, *9*, 1173.
35. Huisgen, R. *Pure Appl. Chem.* **1989**, *61*, 613.
36. Huisgen, R.; Szeimies, G.; Möbius, L. *Chem. Ber.* **1967**, *100*, 2494.
37. Tornøe, C. W.; Christensen, C.; Meldal, M. *J. Org. Chem.* **2002**, *67*, 3057.
38. Rostovtsev, V. V.; Green, L. G.; Fokin, V. V.; Sharpless, K. B. *Angew. Chem., Int. Ed.* **2002**, *41*, 2596.
39. Kolb, H. C.; Finn, M. G.; Sharpless, K. B. *Angew. Chem., Int. Ed.* **2001**, *40*, 2004.
40. Stille, J. K.; Groh, B. L. *J. Am. Chem. Soc.* **1987**, *109*, 813.
41. Mapp, A. K.; Heathcock, C. H. *J. Org. Chem.* **1999**, *64*, 23.
42. Dabdoub, M. J.; Dabdoub, V. B.; Baroni, A. C. M. *J. Am. Chem. Soc.* **2001**, *123*, 9694.
43. Bialy, L.; Waldmann, H. *Angew. Chem., Int. Ed.* **2002**, *41*, 1748.
44. Bialy, L.; Waldmann, H. *Chem. Eur. J.* **2004**, *10*, 2759.
45. Ishiyama, M.; Miyazono, Y.; Sasamoto, K.; Ohkura, Y.; Ueno, K. *Talanta* **1997**, *44*, 1299.
46. Tominaga, H.; Ishiyama, M.; Ohseto, F.; Sasamoto, K.; Hamamoto, T.; Suzuki, K.; Watanabe, M. *Anal. Commun.* **1999**, *36*, 47.
47. Choudhuri, S. D.; Ayers, S.; Soine, W. H.; Reynolds, K. A. *J. Antibiot.* **2005**, *58*, 573.
48. Xing, Y.; Xu, Y.; Chen, Y.; Jeffrey, P. D.; Chao, Y.; Lin, Z.; Li, Z.; Strack, S.; Stock, J. B.; Shi, Y. *Cell* **2006**, *127*, 341.
49. Fushimi, S.; Nishikawa, S.; Shimazu, A.; Seto, H. *J. Antibiot.* **1989**, *42*, 1019.
50. Fushimi, S.; Furihata, K.; Seto, H. *J. Antibiot.* **1989**, *42*, 1026.
51. Umezawa, I.; Komiyama, K.; Oka, H.; Okada, K.; Tomisaka, S.; Miyano, T.; Takano, S. *J. Antibiot.* **1984**, *37*, 706.
52. Longley, R. E.; Caddigan, D.; Harmody, D.; Gunasekera, M.; Gunasekera, S. P. *Transplantation* **1991**, *52*, 650.
53. Longley, R. E.; Caddigan, D.; Harmody, D.; Gunasekera, M.; Gunasekera, S. P. *Transplantation* **1991**, *52*, 656.
54. Kobayashi, S.; Tsuchiya, K.; Harada, T.; Nishide, M.; Kurokawa, T.; Nakagawa, T.; Shimada, N.; Kobayashi, K. *J. Antibiot.* **1994**, *47*, 697.
55. Kobayashi, S.; Tsuchiya, K.; Kurokawa, T.; Nakagawa, T.; Shimada, N.; Iitaka, Y. *J. Antibiot.* **1994**, *47*, 703.
56. Diot, J.; García-Moreno, M. I.; Gouin, S. G.; Ortiz Mellet, C.; Haupt, K.; Kovensky, J. *Org. Biomol. Chem.* **2009**, *7*, 357.